SUPPLEMENTAL INFORMATION

ATF3 Coordinates Serine And Nucleotide Metabolism To Drive Cell Cycle Progression In Acute Myeloid Leukemia

Daniela Di Marcantonio, Esteban Martinez, Joice S. Kanefsky, Jacklyn M. Huhn, Rashid Gabbasov, Anushk Gupta, John J. Krais, Suraj Peri, YinFei Tan, Tomasz Skorski, Adrienne Dorrance, Ramiro Garzon, Aaron R. Goldman, Hsin-Yao Tang, Neil Johnson, and Stephen M. Sykes

Figure S1

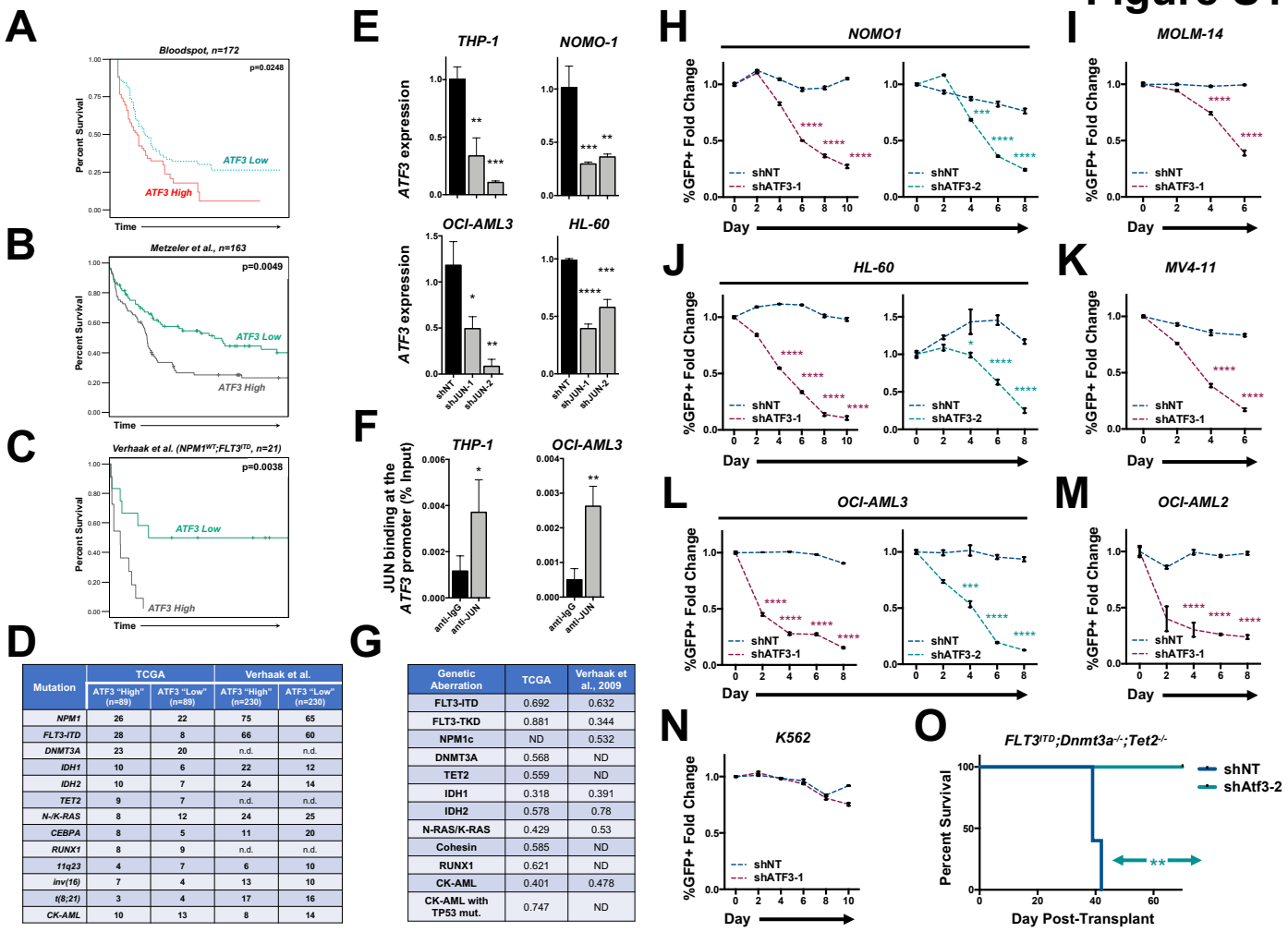

D

Mutation	TCGA		Verhaak et al.	
	ATF3 "High" (n=89)	ATF3 "Low" (n=89)	ATF3 "High" (n=230)	ATF3 "Low" (n=230)
NPM1	26	22	75	65
FLT3-ITD	28	8	66	60
DNMT3A	23	20	n.d.	n.d.
IDH1	10	6	22	12
IDH2	10	7	24	14
TET2	9	7	n.d.	n.d.
N-/K-RAS	8	12	24	25
CEBPA	8	5	11	20
RUNX1	8	9	n.d.	n.d.
11q23	4	7	6	10
inv(16)	7	4	13	10
t(8;21)	3	4	17	16
CK-AML	10	13	8	14

G

Genetic Aberration	TCGA	Verhaak et al., 2009
FLT3-ITD	0.692	0.632
FLT3-TKD	0.881	0.344
NPM1c	ND	0.532
DNMT3A	0.568	ND
TET2	0.559	ND
IDH1	0.318	0.391
IDH2	0.578	0.78
N-RAS/K-RAS	0.429	0.53
Cohesin	0.585	ND
RUNX1	0.621	ND
CK-AML	0.401	0.478
CK-AML with TP53 mut.	0.747	ND

Figure S1 related to Figure 1. (A-C) Kaplan-Meier survival of AML patients divided by low vs high *ATF3* expression from the AML-TGCA dataset (A), from the German AMLCG 1999 dataset (Metzeler et al., 2008) (B) or from Verhaak et al., 2009 – specifically those AMLs that are wild type for NPM1 (NPM1 wt) and carry a $FLT3^{ITD}$ (C). ATF3 high represents patients expressing ATF3 at levels higher than the median and ATF3 low represents patients with ATF3 expression below the median. **(D)** Table enumerating the number of indicated mutations in high versus low ATF3 expressers from the TCGA and Verhaak et al. gene expression datasets. **(E)** qPCR analysis of JUN and ATF3 expression in shNT-, shJUN-1- and shJUN-2-expressing THP-1 (top, left panel), NOMO-1 (top, right panel), OCI-AML3 (bottom, left panel), and HL-60 (bottom, right panel) cells. Data represent the mean ± SD of three technical replicates. **(F)** qPCR quantification of JUN binding at the ATF3 promoter from anti-IgG and anti-JUN ChIP analyses in THP-1 (top panel) and OCI-AML3 (bottom panel) cells. Data are presented as the % of input and represent the mean ± SD of three technical replicates. **(G)** Table enumerating the Spearman correlation coefficients of JUN and ATF3 expression in the indicated mutations from the TCGA and Verhaak et al. gene expression datasets. **(H)** NOMO-1, **(I)** MV4-11, **(J)** HL-60, **(K)** MOLM-14, **(L)** OCI-AML3, **(M)** OCI-AML2, and **(N)** K562 expressing control- (shNT) or ATF3-targeting (shATF3-1 or -2) were assessed for an *in vitro* competitive growth assay as assessed in Figure 1A. **(O)** Kaplan–Meier survival curve analysis of mice transplanted with mouse $FLT3^{ITD}$;$Dnmt3a^{-/-}$; $Tet2^{-/-}$ leukemia cells expressing either shNT or shAtf3-2 (Log-rank (mantel-cox) test; n=5). Asterisk key = *P ≤ 0.05; **P ≤ 0.01; ***P ≤ 0.001; ****P ≤ 0.0001.

Figure S2

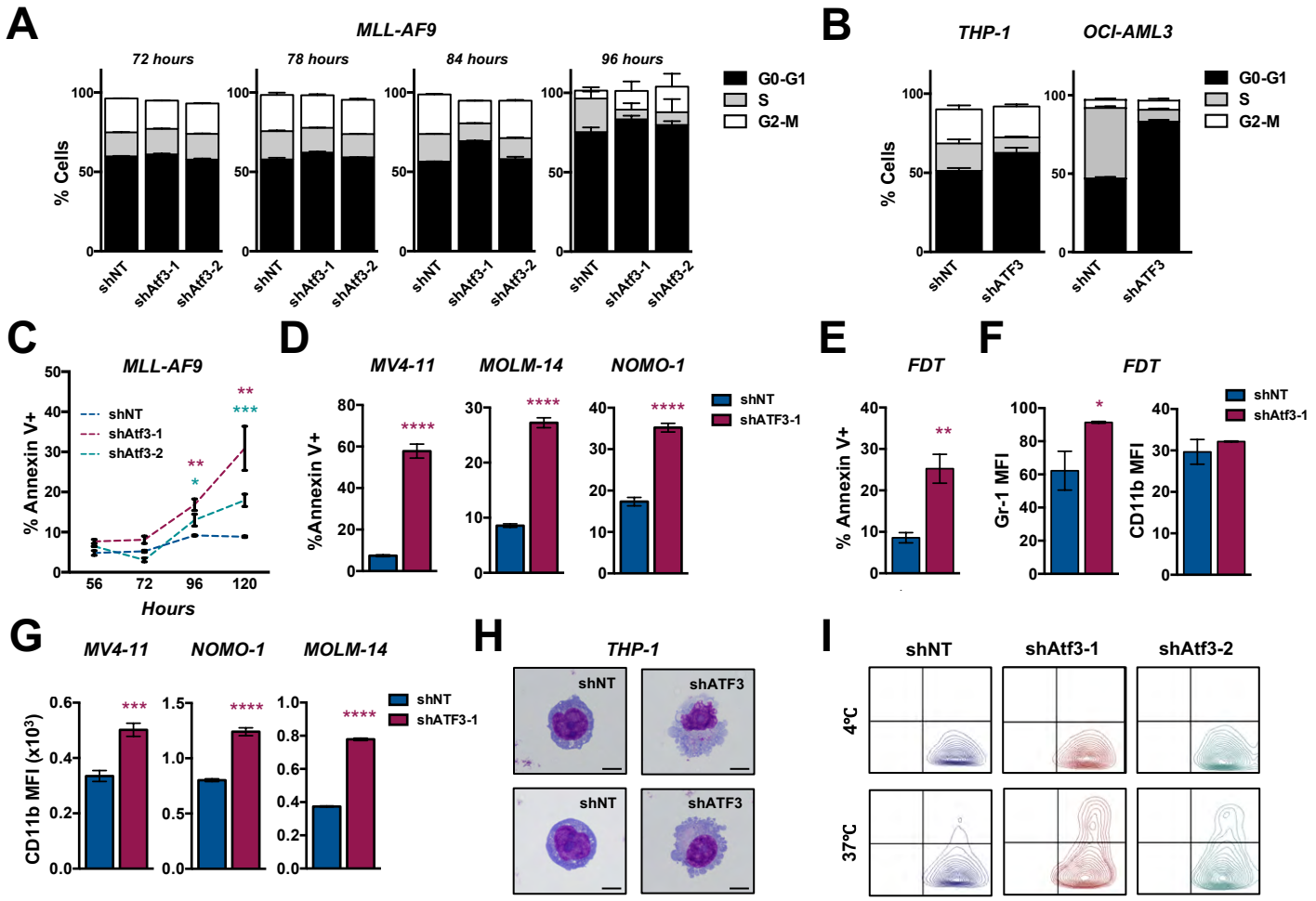

Figure S2 related to Figure 2. (A) MLL-AF9 cells expressing shNT, shAtf3-1 or shAtf3-2 were sorted at 72-, 78-, 84- and 96-hours post-transduction and then fixed and stained with PI and then analyzed by flow cytometry. Data represent the mean ± SD of three technical replicates. **(B)** THP-1 and OCI-AML3 infected with lentiviruses expressing shNT or shATF3-1 were sorted and stained with PI and then analyzed by flow cytometry. Data represent the mean ± SD of three technical replicates. **(C)** MLL-AF9 cells expressing shNT, shAtf3-1 or shAtf3-2 were analyzed by flow cytometry for the percentage of cells positive for Annexin-V staining (% Annexin-V+) at the indicated times post-transduction. **(D)** Flow cytometric analysis of the %Annexin V+ cells in MV4-11, MOLM-14 and NOMO-1 expressing shNT or shATF3-1 at 8-days post-transduction. Data represent the mean ± SD of three technical replicates. **(E & F)** FLT3^{ITD}; Dnmt3a$^{-/-}$; Tet2$^{-/-}$ (FDT) cells were transduced with shNT or shAtf3-1 and analyzed by flow cytometry for the %Annexin V+ cells (E) and Gr1 and CD11b MFI (F). Data represent the mean ± SD of three technical replicates. **(G)** MV4-11, NOMO-1 and MOLM-14 expressing shNT or shATF3-1 were analyzed for CD11b MFI by flow cytometry. Data represent the mean ± SD of three technical replicates. **(H)** Wright-Giemsa staining of THP-1 cells infected with shNT or shATF3-1 and analyzed 7 days after infection (100X magnification - bar = 200µm). **(I)** Contour plot analysis showing the gating strategy for the phagocytosis assay shown in figure 2F. Asterisk key = *P ≤ 0.05; **P ≤ 0.01; ***P ≤ 0.001; ****P ≤ 0.0001.

Figure S3

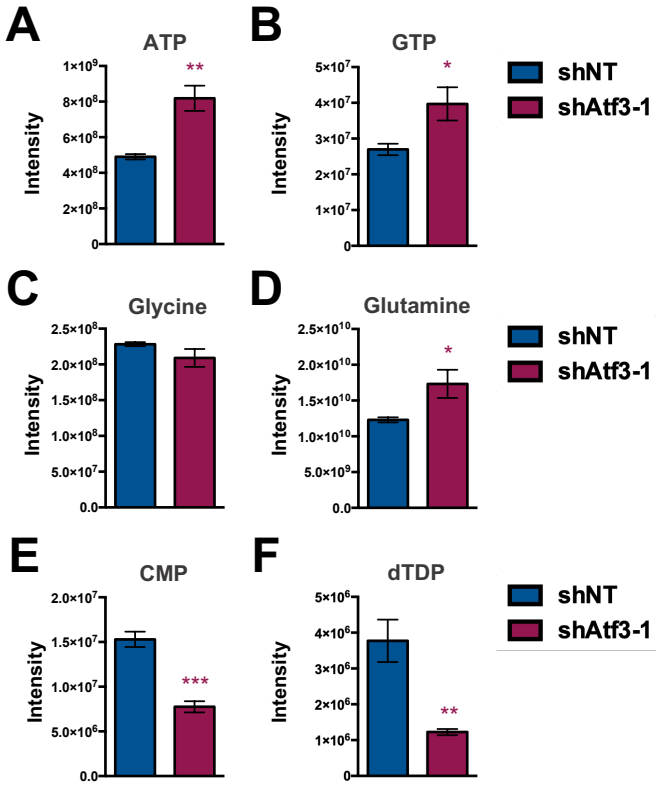

Figure S3 related to Figure 4. (A-F) Steady-state levels of various purine synthesis pathway metabolites extracted from shNT- or shAtf3-1-expressing MLL-AF9 at 72-hours post-transduction: **(A)** ATP, **(B)** GTP, **(C)** Glycine, **(D)** Glutamine, **(E)** CMP, **(F)** dTDP.

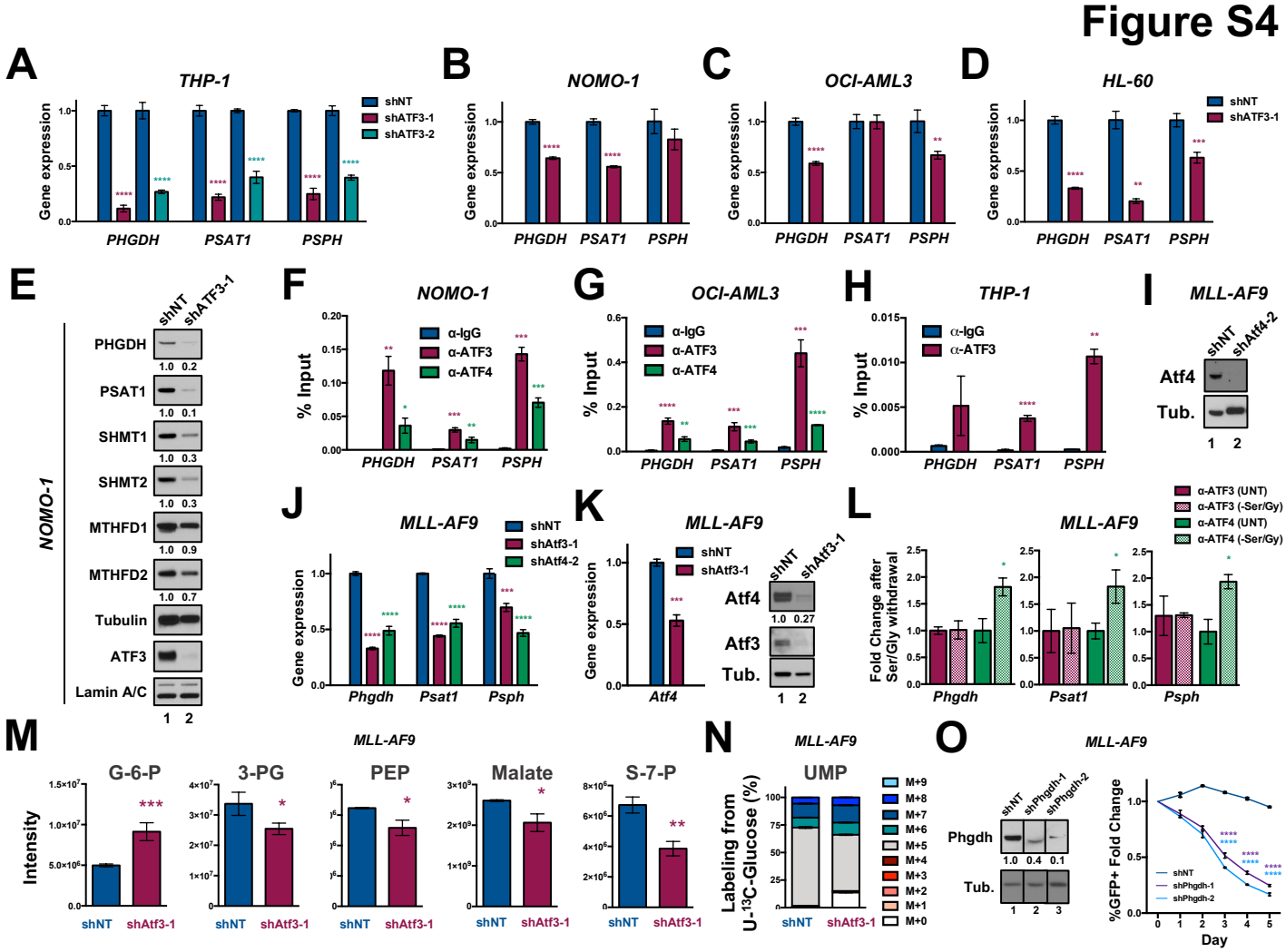

Figure S4 related to Figure 5. (A-D) qPCR analysis of steady-state levels of *PHGDH*, *PSAT1* and *PSPH* mRNA in THP-1 **(A)**, NOMO-1 **(B)**, OCI-AML3 **(C)** and HL-60 **(D)** cells expressing the indicated shRNAs. Data represent the mean ± SD of three technical replicates. **(E)** Western blot analysis of FACS-sorted GFP$^+$ NOMO-1 cells expressing shNT or shATF3 at 96-hours post-transduction with the indicated antibodies. Proteins levels were quantified and normalized to tubulin expression. **(F & G)** qPCR quantification of ATF3 and ATF4 binding at *PHGDH, PSAT1* and *PSPH* promoters from anti-IgG, -ATF3 or -ATF4 ChIP analyses in NOMO-1 (F) and OCI-AML3 (G). The approximate promoter regions are: *PHGDH* (0 - +1000); *PSAT1* (-500 - +500); *PSPH* (+9000 - +10000). Data are presented as the % of input and represent the mean ± SD of three technical replicates. **(H)** qPCR quantification of ATF3 binding at *PHGDH, PSAT1* and *PSPH* promoters from anti-IgG or -ATF3 ChIP analyses in THP-1 cells. Data represent the mean ± SD of three technical replicates. **(I)** Western blot analysis of FACS-sorted GFP$^+$ MLL-AF9 leukemia cells expressing shNT or shAtf4-2 at 48-hours post-transduction with the indicated antibodies. **(J)** qPCR analysis of *Phgdh*, *Psat1* and *Psph* in shNT-, shAtf3-1- and shAtf4-2-expressing MLL-AF9 cells at 48 hours post-transduction. Data represent the mean ± SD of three technical replicates. **(K)** shNT- and shAtf3-1-expressing MLL-AF9 cells were assessed for Atf4 mRNA expression and 48-hours post-transduction (left panel) and Atf4 protein levels and 72-hours post-transduction (right panel). mRNA data represent the mean ± SD of three technical replicates. **(L)** qPCR quantification of anti-ATF3 or -ATF4 ChIP samples from MLL-AF9 cells cultured in serine/glycine-deficient or regular media with primers amplifying regions of the *Phgdh, Psat1*, and *Psph* genes. Data are presented as the fold change of ATF3 or ATF4 binding in MLL-AF9 cells cultured in serine/glycine-deficient divided regular media and represent the mean ± SD of three technical replicates. **(M)** Steady-state levels of various purine synthesis pathway metabolites extracted from shNT- or shAtf3-1-expressing MLL-AF9 at 72-hours post-transduction: Glucose-6-phosphate (G-6-P), 3-phosphoglycerate (3-PG), phosphoenolpyruvate (PEP), Malate, or sedoheptulose-7-phosphate (S-7-P). **(N)** shNT

or shAtf3-1-expressing MLL-AF9 at 48 hours post-transduction were cultured for 24 hours with U-^{13}C-glucose and metabolites were subsequently extracted and analyzed by LC-MS/MS. Isotopologue distribution (%) of the total steady-state levels of UMP. **(O)** *Left panel,* western blot analysis of MLL-AF9 cells expressing control shRNA (shNT) or mouse Phgdh targeting (shPhgdh-1 and -2) shRNAs. This image is a composite of three objects taken from the same western blot micrograph. The three separate micrograph divisions are demarcated by black lines. *Right panel, in vitro* competitive growth curve of MLL-AF9 cells expressing shNT, shPhgdh-1 or shPhgdh-2. Percentage of GFP-positive (%GFP+) cells were evaluated at the indicated time points by flow cytometry and plotted as the fold change in %GFP+ compared to the %GFP+ at day 2 post-transduction (day 0 in the figure). Data represent the mean ± SD of three technical replicates. Asterisk key = *P ≤ 0.05; **P ≤ 0.01; ***P ≤ 0.001; ****P ≤ 0.0001.

Figure S5

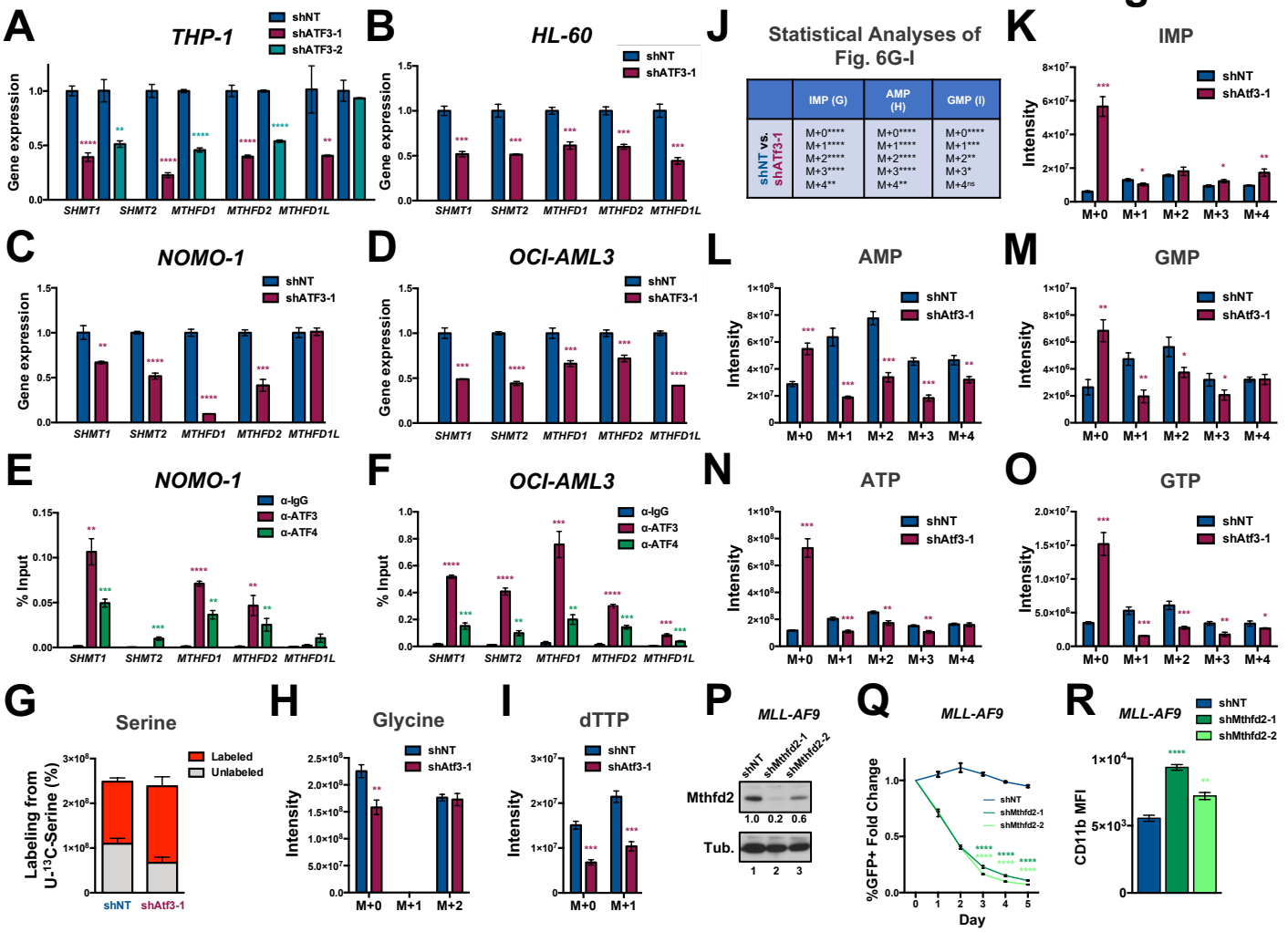

Figure S5 related to Figure 6. (A-D) qPCR analysis of one-carbon metabolism enzymes of THP1 **(A)**, HL-60 **(B)**, NOMO-1 **(C)** and OCI-AML3 **(D)** cells expressing the indicated shRNAs. Data are represented as mean ± SD of three replicates. **(E & F)** qPCR quantification of ATF3 and ATF4 binding at *SHMT1, SHMT2, MTHFD1, MTHFD2* and *MTHFD1L* promoters from anti-IgG, -ATF3 or -ATF4 ChIP analyses in NOMO-1 (E) and OCI-AML3 (F). The approximate promoter regions are: SHMT1 (+500 - +1500); SHMT2 (0 - +1000); MTHFD1 (-500 - +500); MTHFD2 (-500 - +500); MTHFD1L (0 - +1000). Data are presented as the % of input and represent the mean ± SD of three technical replicates. From the experiment presented in Figure 6: **(G)** Quantification and statistical analysis of the total steady-state levels of serine levels (bar magnitudes) in shNT and shAtf3-1-expressing MLL-AF9 cells. The unlabeled fraction (grey) represents the total steady-state levels of M+0 metabolites and the labeled fractions (red) represent the total steady-state levels of combined isotopologues (the sum of M+1, M+2 and M+3). **(H)** Steady-state levels of unlabeled (M+0) and labeled (M+2) glycine. **(I)** Steady-state levels of unlabeled (M+0) and labeled (M+1) dTTP. **(J)** Table summarizing the statistical analyses of the data presented in Figure 6G-I. **(K-O)** Steady-state levels of unlabeled (M+0) and labeled (M+1, M+2, M+3, M+4) isotopologues of: IMP (K), AMP (L), GMP (M), ATP (N) and GTP (O). **(P)** Western blot analysis of MLL-AF9 cells expressing control shRNA (shNT) or mouse Mthfd2 targeting (shMthfd2-1 and -2) shRNAs with the indicated antibodies. **(Q)** *In vitro* competitive growth curve of MLL-AF9 cells expressing shNT, shMthfd2-1 or shMthfd2-2. Percentage of GFP-positive (%GFP+) cells were evaluated at the indicated time points by flow cytometry and plotted as the fold change in %GFP+ compared to the %GFP+ at day 2 post-transduction (day 0 in the figure). **(R)** MLL-AF9 cells expressing shNT, shMthfd2-1 or shMthfd2-2 were analyzed by flow cytometry for CD11b expression (MFI). Data represent the mean ± SD of three technical replicates. Asterisk key = *P ≤ 0.05; **P ≤ 0.01; ***P ≤ 0.001; ****P ≤ 0.0001.

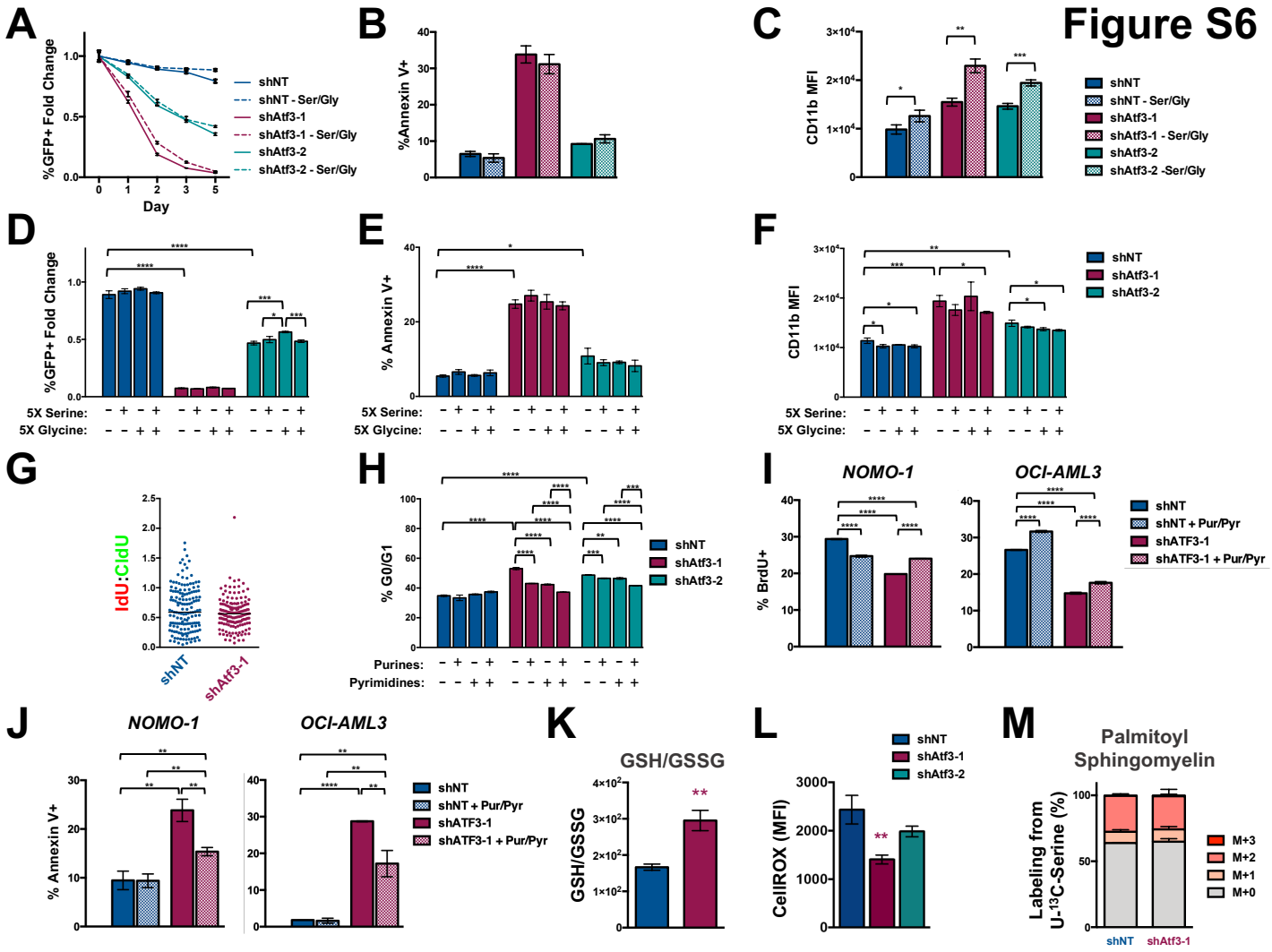

Figure S6 related to Figure 7. (A) MLL-AF9 cells expressing shNT, shAtf3-1 or shAtf3-2 were cultured in either regular media of serine/glycine-deficient and then assessed for changes in % GFP+ by flow cytometry at the indicated time points. Data is presented as the fold change in %GFP+ compared to the %GFP+ at day 2 post-transduction (day 0 in the figure) and represent the mean ± SD of three technical replicates. **(B & C)** MLL-AF9 cells expressing shNT, shAtf3-1 or shAtf3-2 were cultured in either regular media of serine/glycine-deficient and then assessed by flow cytometry for: %Annexin-V+ at 5 days post-transduction (B) or CD11b at 4 days post-transduction (C). Data represent the mean ± SD of three technical replicates. **(D-F)** MLL-AF9 cells expressing shNT, shAtf3-1 or shAtf3-2 were cultured in either regular media, media supplemented with 5X serine, 5X glycine or 5X serine + 5X glycine and then assessed by flow cytometry for: Fold change %GFP+ at 5 days post-transduction, (D) %Annexin-V+ at 5 days post-transduction (E) or CD11b at 4 days post-transduction (F). Data represent the mean ± SD of three technical replicates. **(G)** Analysis of DNA fiber lengths presented as the IdU/CldU length ratio, black bar indicates median values. **(H)** Quantification of percentage of cells in G0/G1 (%G0/G1) from data present in Figure 7D and E. Data represent the mean ± SD of three technical replicates. **(I and J)** NOMO1 and OCI-AML3 cells expressing control or ATF3-targeting shRNAs (shATF3-1) were cultured with vehicle of 12.5 μM of each 2'-deoxyadenosine and 2'-deoxyguanosine, 2'-deoxycytosine and 2'-deoxyuridine 5'-monophosphate and then assessed for: (**I**) %BrdU (NOMO-1, *left panel* and OCI-AML3, *right panel*) or (**J**) %Annexin V+ (NOMO-1, *left panel* and OCI-AML3, *right panel*). **(K)** Ratio of reduced-to-oxidized (GSH/GSSG) steady-state levels of glutathione in shNT- or shAtf3-1-expressing MLL-AF9. **(L)** MLL-AF9 cells expressing NT, Atf3-1 or Atf3-2 shRNAs were stained with CellROX Deep Red and analyzed by flow cytometry at 4 days post-transduction. *Left*, the average MFI of CellROX staining in live cells; *right*, representative histogram plot of a single experiment. **(M)** Isotopologue distribution (%) of the total steady-state levels of

Palmitoyl Sphingomyelin in shNT- or shAtf3-1-expressing MLL-AF9. Asterisk key = *P ≤ 0.05; **P ≤ 0.01; ***P ≤ 0.001; ****P ≤ 0.0001.

Table S1

TUHS #	Accession #	NPM1	FLT3-ITD	ASXL1	RUNX1	TET2	DNMT3A	IDH1
TUHS-AML-002	U-12-0954	wt	ITD	wt	**A343AG or A370AG**	wt	wt	**R132H**
TUHS-AML-0014	U-17-0754	W288s fs	wt	N986S	wt	Q461*; K1321 fs	wt	wt
TUHS-AML-0015	U-17-2361	W288s fs	ITD	G646 fs	wt	Q743*	R882H	wt

*fs = frame shift

Table S1 related to Figure 1. Annotation of mutations found in the patient samples presented in Figure 1E.

Table S2

qPCR Primers		
Gene		**Sequence (5' → 3')**
Phgdh	Forward	ATGGCCTTCGCAAATCTGC
	Reverse	AGTTCAGCTATCAGCTCCTCC
Psat1	Forward	CAGTGGAGCGCCAGAATAGAA
	Reverse	CCTGTGCCCCTTCAAGGAG
Psph	Forward	AGGAAGCTCTTCTGTTCAGCG
	Reverse	GAGCCTCTGGACTTGATCCC
Shmt1	Forward	CAGGGCTCTGTCTGATGCAC
	Reverse	CGTAACGCGCTCTTGTCAC
Shmt2	Forward	TGGCAAGAGATACTACGGAGG
	Reverse	GCAGGTCCAACCCCATGAT
Mthfd1	Forward	GGGAATCCTGAACGGGAAACT
	Reverse	TGAGTGGCTTTGATCCCAATC
Mthfd2	Forward	AGTGCGAAATGAAGCCGTTG
	Reverse	GACTGGCGGGATTGTCACC
Mthfd1l	Forward	GCATGGCCTTACCCTTCAGAT
	Reverse	GTACGAGCTTCCCCAGATTGA
ChIP Primers		
Gene		**Sequence (5' → 3')**
Phgdh	Forward	TGGGCAGGGTTCTCGATCTC
	Reverse	AATCAAAAGGAGACTGTTGGCG
Psat1	Forward	CTTCCATGGTGCTAAGGCGA
	Reverse	GACTCCGATAGTGAGCGTGG
Psph	Forward	CAGAGAGGAGATAGCCGTGG
	Reverse	ACAGGTACCGGAACCGAGAA
Shmt1	Forward	GGATCACAGTAGTGCATCCCC
	Reverse	TGGACTGACTTTACCCCTAGGAA
Shmt2	Forward	GTTCTTACCCGAGTGGTCCG
	Reverse	AGAGCAGCTGGTTTTCGACC
Mthfd1	Forward	GGAGAAGCCAGTACGATCCA
	Reverse	CTGAGCAAGTTTGCGTGACC
Mthfd1l	Forward	AGATACTGCTGCACCGGAAC
	Reverse	TAGGTCTAGGCGTACGGTCC

Table S2 related to STAR methods. List of the qPCR and ChIP primers used through the study to recognize the indicated mouse gene targets.

Table S3

qPCR Primers		
Gene		**Sequence (5' → 3')**
PHGDH	Forward	CTGCGGAAAGTGCTCATCAGT
	Reverse	TGGCAGAGCGAACAATAAGGC
PSAT1	Forward	TGCCGCACTCAGTGTTGTTAG
	Reverse	GCAATTCCCGCACAAGATTCT
PSPH	Forward	GAGGACGCGGTGTCAGAAAT
	Reverse	GGTTGCTCTGCTATGAGTCTCT
SHMT1	Forward	CTGGCACAACCCCTCAAAGA
	Reverse	AGGCAATCAGCTCCAATCCAA
SHMT2	Forward	CCCTTCTGCAACCTCACGAC
	Reverse	TGAGCTTATAGGGCATAGACTCG
MTHFD1	Forward	GCGCCAGCAGAAATCCTGA
	Reverse	AGGTACTTGCTCCTTCAACTGA
MTHFD2	Forward	AGGACGAATGTGTTTGGATCAG
	Reverse	GGAATGCCAGTTCGCTTGATTA
MTHFD1L	Forward	CTGCCTTCAAGCCGGTTCTT
	Reverse	TTTCCTGCATCAAGTTGTCGT
R18S	Forward	GCCCCTGTAATTGGAATGAGTC
	Reverse	CCAAGATCCAACTACGAGCTT
ChIP Primers		
Gene		**Sequence (5' → 3')**
PHGDH	Forward	TCTGATGCAAGACTGCTCCG
	Reverse	GTCTGGTCACTCCCAACCAG
PSAT1	Forward	AGGAGCAACTGCTTCGACTC
	Reverse	CCTGCGCTAATTGGTTCGC
PSPH	Forward	GGGGATTGTTCCAATCTTGCAC
	Reverse	CCTGTTGCCAAACAGCATGA
SHMT1	Forward	GATTGAAGGCCCGCATCTGT
	Reverse	CTTGGCTTCGAGATTCCGGG
SHMT2	Forward	GAGTTTTCGGCCTGGTCTCA
	Reverse	GGATCTGCCCGAGAGTAAGC
MTHFD1	Forward	TGGTGCCAACTCATTAGGGG
	Reverse	TACTGGATCCCCCGTTCTCC
MTHFD2	Forward	TCTGATGCAAGACTGCTCCG
	Reverse	GTCTGGTCACTCCCAACCAG
MTHFD1L	Forward	AGGAGCAACTGCTTCGACTC-
	Reverse	CCTGCGCTAATTGGTTCGC

Table S3 related to STAR methods. List of the qPCR and ChIP primers used through the study to recognize the indicated human gene targets.